Hard x-ray phase contrast imaging of black lipid membranes

A. Beerlink, M. Mell, M. Tolkiehn, and T. Salditt

Citation: Applied Physics Letters **95**, 203703 (2009); doi: 10.1063/1.3263946
View online: http://dx.doi.org/10.1063/1.3263946
View Table of Contents: http://scitation.aip.org/content/aip/journal/apl/95/20?ver=pdfcov
Published by the AIP Publishing

Hard x-ray phase contrast imaging of black lipid membranes

A. Beerlink,[a] M. Mell, M. Tolkiehn, and T. Salditt[a]
Institut für Röntgenphysik, Universität Göttingen, Friedrich-Hund-Platz 1, 37077 Göttingen, Germany

(Received 11 August 2009; accepted 8 October 2009; published online 19 November 2009)

We report hard x-ray phase contrast imaging of black lipid membranes, freely suspended over a micromachined aperture in an aqueous solution. Biomolecular and organic substances can thus be probed in hydrated environments by parallel beam propagation imaging, using coherent multi-kilo-electronvolt x-ray radiation. The width of the thinning film can be resolved from analysis of the intensity fringes in the Fresnel diffraction regime down to about 200 nm. The thinning process, in which solvent is expelled from the space in between two opposing monolayers, is monitored, and the domain walls between coexisting domains of swollen and thinned membrane patches are characterized. © *2009 American Institute of Physics*. [doi:10.1063/1.3263946]

Membranes are considered as the most important interfaces in biology, and can be visualized under physiological conditions by optical techniques such as phase contrast and fluorescence light microscopy. While the contour lines and large lateral domains of biological membranes can be imaged, the density profile of the membrane and associated changes cannot be resolved by visible light. On molecular length scales lipid bilayer model membranes have been studied by x-ray and neutron scattering and reflectivity.[1–4] In these studies, the structural information is averaged over large ensembles, e.g., in isotropic suspensions of several microliters or on planar model bilayers on the order of cm^2. Between scattering studies, on one hand, carried out over large ensembles, and microscopic studies, on the other hand, there is a large gap concerning resolution, interaction volume and complexity of the system studied. For example, scattering requires relatively simple and defect-free model systems with well separated length scales, whereas structure in functional context should be probed by *in situ* setups in samples with a larger hierarchy of length scales.

We have recently adapted a well known setup of membrane electrophysiology, i.e., single freely suspended bilayers spanned in between two separated, aqueous compartments (differing in pH, ion concentrations, etc.), to *in situ* x-ray structural studies.[5] These so-called black lipid membranes (BLM) are an established model system in membrane biophysics,[6,7] allowing studies of functional transport across the bilayer at controlled compositional and environmental parameters, such as protein concentration, ion strength, pH, and electrical field.

Here we image black lipid membranes based on hard x-ray Fresnel diffraction (propagation imaging), with phase contrast arising from free space propagation of the beam traversing the sample.[8–13] We show that for the studied membranes a simplified but extendable model can be used to quantitatively monitor the thickness and its changes during the thinning process of BLMs.

The experimental scheme is shown in Fig. 1. BLMs of 1,2-diphytanoyl-sn-glycero-3-phosphocholine were prepared by the painting method of Mueller and Rudin,[6] using n-decane (Sigma-Aldrich, Germany) (5 mg/ml) as a solvent, see[5] and EPAPS. Images shown here have been recorded at the ID10C (Troika III) undulator station of ESRF (Grenoble, France). Similar and consistent results have been obtained independently at the bending magnet beamline BM05 of ESRF, under comparable optical parameters.[5] The beam was monochromatized by a diamond-(111)-crystal monochromator to 20.92 keV with a bandpass of $\frac{\Delta\lambda}{\lambda}=3.7\cdot10^{-5}$. The (unfocused) beam size at the sample was 1 mm × 1 mm, as controlled by a series of high quality motorized slits optimized for coherent scattering. Images were taken at the three different propagation distances $z=0.06$, 2.18, and 3.63 m, respectively, between sample and detector (also called defocus distance), using a Sensicam 12-bit charge coupled device camera (PCO Imaging, Germany) with 1240 (h) × 1024 (v) pixels and a pixel size of 6.7 μm × 6.7 μm. At the detector, a scintillation foil [9.9 μm europium doped lutetium aluminum garnet (LuAG:Eu) on 170 μm undoped yttrium aluminum garnet (YAG)], imaged by a 10× objective onto the detector, was used.

The data reduction yields a one-dimensional (1D) intensity profile $I(x,z)$, see Fig. 2, in the detector plane D (SOM). We consider the measured $I(x,z)$ as the squared output of the 1D Fresnel operator acting on the 1D optical transmission function, which for a pure phase object is $T(x)=e^{i\varphi(x)}$. $T(x)$

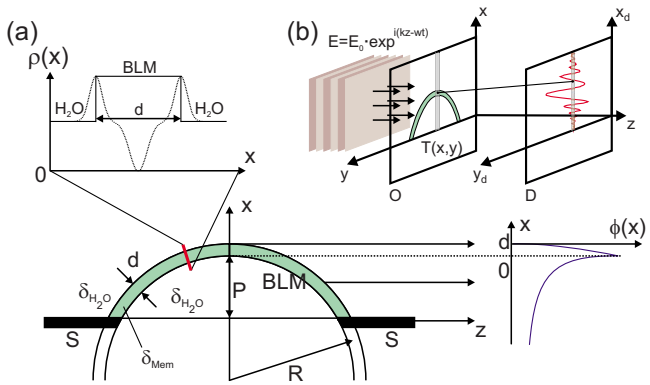

FIG. 1. (Color online) (a) Experimental setup: A parallel hard x-ray wave front (E) coherently illuminates a spherically BLM with thickness d, spanned over a micromachined hole in a solid substrate S, located in the object plane O. (b) The sample is described by a transmission function $T(x,y)$ obtained by projection of the electron density $\rho(x)$ along the z-axis. After free space propagation of the exit wave over a distance z along the optical axis, a Fresnel interference pattern is recorded in the detector plane D, representing a phase contrast image of the projected density profile.

[a]Electronic addresses: abeerli@gwdg.de and tsaldit@gwdg.de.

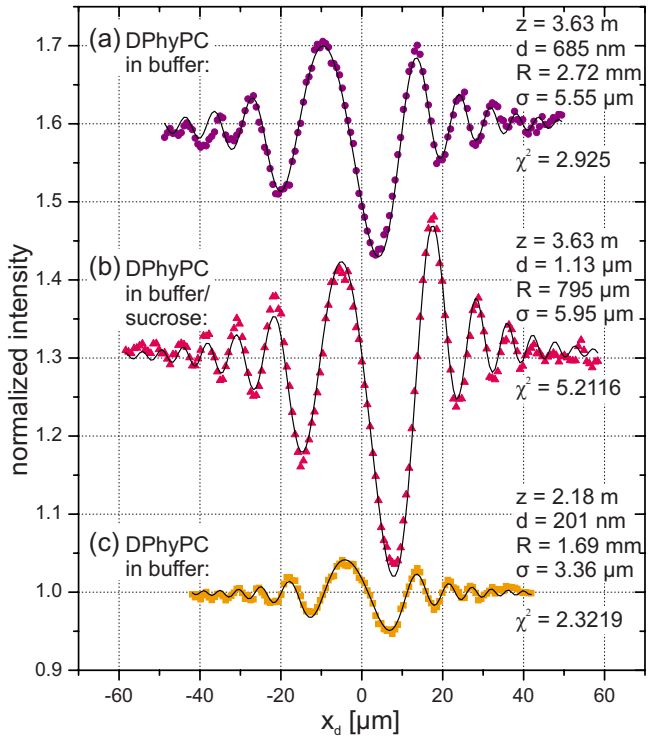

FIG. 2. (Color online) Exemplary intensity profiles (dotted) along with the fits (solid line) for two different propagation distances (a), (b) 3.63 m, and (c) 2.18 m (shifted for clarity). (b) Shows the profile extracted from a BLM in a sucrose-buffer $[1:1(w/w)]$ solution. The fitting results are shown in the insets.

reflects the structure of the membrane patch along its local normal axis in O. The accumulated phase shift difference with respect to the empty space of the wave traversing the membrane is $\varphi(x)=-k\int_L \delta(x,z)dz$, where $n=1-\delta$ is the real part of the index of refraction, $k=2\pi/\lambda$ the wave number, and $L(x)$ the interaction length. The projection approximation and the disregard of absorption is well justified for the chosen photon energy and weakly scattering objects of the given size. For simplicity, we first consider the simplest membrane structure with constant electron density, which is well suited for black lipid membranes swollen with organic solvent before the thinning transition takes place. The phase profile behind the object (exit wave) is then simply $\varphi(x)\simeq -k\Delta\delta L(x)$, where $\Delta\delta$ is the refractive index difference with respect to the surrounding water.[14] The Fresnel operator is given in paraxial approximation by the 1D Fresnel–Kirchhoff equation, for the given propagation distance z:

$$E(x_d,z)=E_0\sqrt{\frac{k}{2\pi z}}e^{-i(\pi/4)}\int_{-\infty}^{\infty}e^{i\varphi(x)}e^{ik(x-x_d)^2/2z}dx. \qquad (1)$$

The prefactor indicates that the contrast for given (fixed) phase profile $\phi(x)$ actually decreases with λ ! By control of membrane curvature, one can always bring the phase shift by tangential beam path through the membrane to an optimum value (Fig. 1), nearly independent of λ, justifying the relatively high photon energy chosen. For numerical computation of $I(x,z)=|E(x,z)|^2$, a box model of $\varphi(x)$ can be used for the central interval of the object plane, where the phase shift $\varphi(x)$ is nonzero. The Fresnel–Kirchhoff integral can then be solved analytically in terms of a sum of Fresnel sine and cosine functions (SOM). To obtain the complete field $E(x)=E_c(x)+E_l(x)+E_r(x)$, the fields $E_l(x)$ and $E_r(x)$ due to the source points in the left and right half-planes have to be added. For these regions constant phase shifts $\varphi_l=\varphi_r=0$ were assumed. The model as used to analyze the set of measured profiles by least-square fitting, is characterized by the following parameters: membrane thickness d, refractive index contrast $\Delta\delta$, and the local radius of curvature R, as well as the propagation distance z and wave number k. d was varied freely in the fit, while $\Delta\delta$ was fixed to the theoretical values of water and lipid/oil, for the given photon energy, which also fixed k. The propagation distance z was measured, but a refinement of the measured values within a reasonable range was allowed during the fit. Before comparing to the measured intensity profiles, the calculated curve was convoluted with a Lorentzian function with width parameter σ taking into account both the point spread function of the detector and the finite lateral coherence length of the x-rays. Note that convolution with a Lorentzian gave slightly better fits than with a Gaussian.

Figure 2 presents examples of the measured Fresnel diffraction profiles (dotted) along with the least-square fits of the model (solid line). The resulting parameters are indicated in the legend. In addition to variation of z, sucrose was added to the buffer solution [2.92 M solid sucrose, Fig. 2(b)], to increase $\Delta\delta$. For all profiles, satisfactory and consistent fits could be obtained. With increasing distance from the optical axis (x), as well as with decreasing propagation distance (z), the intensity oscillates more rapidly, until it is no longer resolved by the detector. The most important length scale of the image formation process is the reduced propagation length $Z=\sqrt{z\lambda}$. For $d\ll Z$, the Fresnel oscillations are described by a superposition of $\sin\chi$ and $\cos\chi$, with $\chi=2\pi x_d^2/Z^2$. The exact superposition is determined by the two parameters d and $\Delta\delta$. At small z, only the main contour is resolved, as is well known for the edge contrast regime of propagation imaging.[15] Membrane thickness values down to $d\simeq 200$ nm could be obtained, before contrast was lost. Note that d changes locally and with time, as the solvent used in painting the lipid membrane over the aperture slowly diffuses out toward the rim over a time scale of minutes, up to hours. The final transition yields a thinned membrane, with $d\simeq 3-4$ nm corresponding to a lipid bilayer.

Figure 3 reflects a membrane state with a coexistence of swollen and thinned regions. In the two-dimensional image (a), the membrane contour appears like a "free arc in air." Close to the so-called Plateau–Gibbs-border solvent accumulates and the local thickness yields a strong phase contrast image, while the thinned region toward the center of the bulged membrane is not visible. Radial cuts, indicated by the lines numbered in (a), are shown with a corresponding, representative least-square fit in (b). Subsequent radial cuts, shown in (a), along the contour length s indicate the decrease of the intensity oscillations. The corresponding thickness values, plotted in (c), follow an empirical *tanh*-profile. This profile is regarded as a domain wall separating a coexisting swollen state (two lipid monolayers swollen with n-decane) and a thinned bilayers state with expelled solvent. In this regime, the noise limits the resolution in d.[14]

In summary, we have shown that a black lipid membrane can be imaged by hard x-ray propagation imaging and that the profile can be analyzed quantitatively in terms of the vertical density profile $\rho(z)$ of the membrane. The case of a

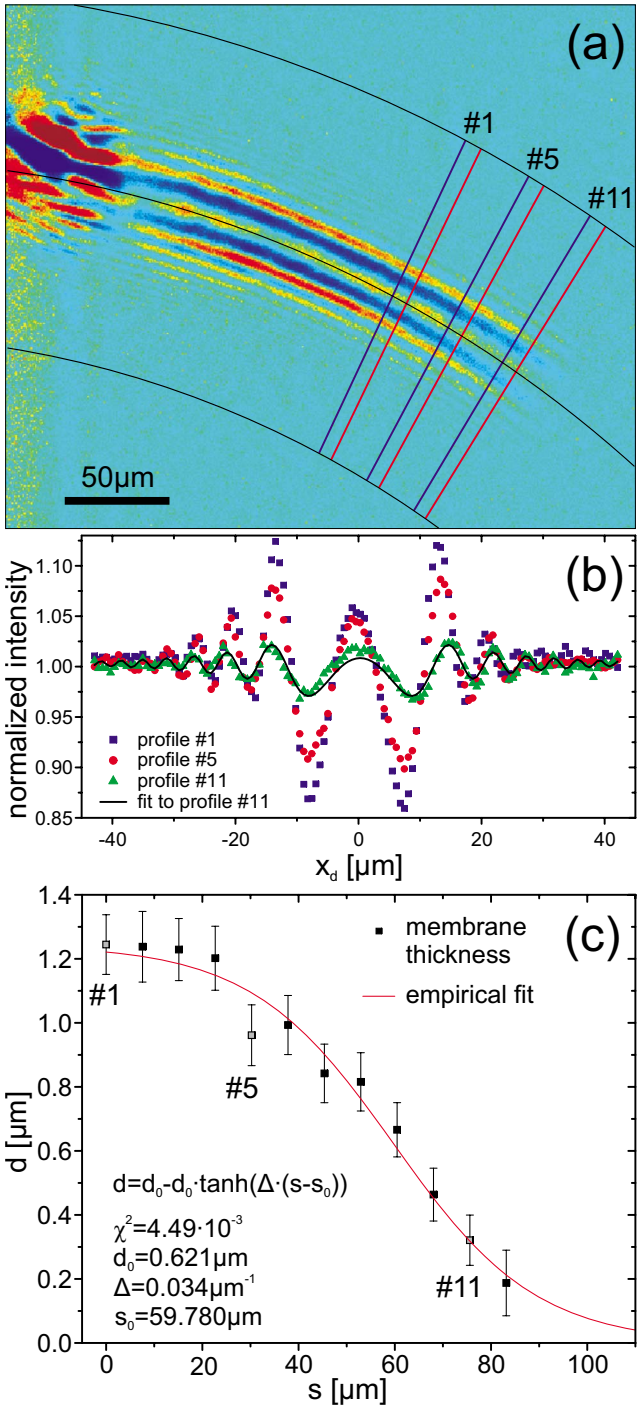

FIG. 3. (Color online) (a) Series of extracted profiles at propagation distance 2.18 m, illustrating the coexistence of swollen and thinned regions. (b) The thinning process progressed from the center of the bulged membrane toward the Plateau–Gibbs-border near the substrate and is accompanied by a loss of contrast in the intensity profiles. (c) The decrease of membrane thickness d as determined from the fits with the contour length s and an empirical fit.

swollen BLM state with excess solvent in between the lipid monolayers was investigated here, along with the thinning process. This state justifies a simplified slab model. However, the model is easily extended to nontrivial profiles $\rho(z)$. In the present experiment, the contrast was not sufficient to image a thinned membrane (bilayer). Thickness values on the order of $d \simeq 200$ nm could already be extracted by quantitative fitting in the current parallel beam setup. By scaling arguments and simulation we have estimated that a native (thinned) bilayer state could be resolved by Fresnel imaging by use of a projection setup with a divergent beam. A sensitivity of below 10 nm can be expected, using a moderate magnification $z_2/z_1 \leq 100$, where z_1 is the distance of the membrane from the focus, e.g., created by compound refractive lenses[16,17] or an x-ray waveguide,[18,19] and z_2 is the distance between the sample and the detector. Disregarding possible radiation damage in such a focused beam, structural changes in the bilayer, e.g., resulting from external fields or ion concentrations in the two compartments, or from transport of molecules through the bilayer may then become accessible. This approach of coherent propagation imaging can thus serve to study the nanoscale structure of individual hydrated biomolecular assemblies.

We acknowledge financial support by Deutsche Forschungsgemeinschaft through SFB755 Nanoscale Photonic Imaging. It is also a pleasure to thank Lutz Wiegert and Anders Madsen for their support at the ID10C.

[1] J. Als-Nielsen and D. McMorrow, *Elements of Modern X-ray Physics* (Wiley, London, 2001).
[2] G. S. Smith, E. B. Sirota, C. R. Safinya, R. J. Plano, and N. A. Clark, Phys. Rev. Lett. **60**, 813 (1988).
[3] C. E. Miller, J. Majewski, T. Gog, and T. L. Kuhl, Phys. Rev. Lett. **94**, 238104 (2005).
[4] E. Nováková, G. Mitrea, C. Peth, J. Thieme, K. Mann, and T. Salditt, BioInterphases **3**, 44 (2008).
[5] A. Beerlink, P.-J. Wilbrandt, E. Ziegler, D. Carbone, T. H. Metzger, and T. Salditt, Langmuir **24**, 4952 (2008).
[6] P. Mueller, D. O. Rudin, H. T. Tien, and W. C. Wescott, Nature (London) **194**, 979 (1962).
[7] H. Tien and A. Ottova-Leitmannova, *Membrane Biophysics* (Elsevier, Amsterdam, 2000).
[8] T. J. Davis, D. Gao, T. E. Gureyev, A. W. Stevenson, and S. W. Wilkins, Nature (London) **373**, 595 (1995).
[9] A. Snigirev, I. Snigireva, V. Kohn, S. Kuznetsov, and I. Schelokov, Rev. Sci. Instrum. **66**, 5486 (1995).
[10] C. Raven, A. Snigirev, I. Snigireva, P. Spanne, A. Souvorov, and V. Kohn, Appl. Phys. Lett. **69**, 1826 (1996).
[11] P. Cloetens, R. Barrett, J. Baruchel, J.-P. Guigay, and M. Schlenker, J. Phys. D **29**, 133 (1996).
[12] S. W. Wilkins, T. E. Gureyev, D. Gao, A. Pogany, and A. W. Stevenson, Nature (London) **384**, 335 (1996).
[13] P. Cloetens, W. Ludwig, J. Baruchel, J.-P. Guigay, P. Pernot-Rejmánkova, M. Salomé-Pateyron, M. Schlenker, J.-Y. Buffière, E. Maire, and G. Peix, J. Phys. D **32**, A145 (1999).
[14] See EPAPS supplementary material at http://dx.doi.org/10.1063/1.3263946 for a detailed description of the theoretical background and for an image series of a thinning BLM.
[15] S. Mayo, T. Davis, T. Gureyev, P. Miller, D. Paganin, A. Pogany, A. Stevenson, and S. Wilkins, Opt. Express **11**, 2289 (2003).
[16] B. Lengeler, C. G. Schroer, M. Richwin, J. Tümmler, M. Drakopoulos, A. Snigirev, and I. Snigireva, Appl. Phys. Lett. **74**, 3924 (1999).
[17] C. G. Schroer, J. Meyer, M. Kuhlmann, B. Benner, T. F. Günzler, B. Lengeler, C. Rau, T. Weitkamp, A. Snigirev, and I. Snigireva, Appl. Phys. Lett. **81**, 1527 (2002).
[18] S. Lagomarsino, A. Cedola, P. Cloetens, S. di Fonzo, W. Jark, G. Soullié, and C. Riekel, Appl. Phys. Lett. **71**, 2557 (1997).
[19] T. Salditt, S. P. Krüger, C. Fuhse, and C. Bähtz, Phys. Rev. Lett. **100**, 184801 (2008).